Research Article

MOLECULAR PAIN

Molecular Pain
Volume 14: 1–12

DOI: 10.1177/1744806918788638
journals.sagepub.com/home/mpx
SAGE

Nonmuscle myosin II isoforms interact with sodium channel alpha subunits

Bhagirathi Dash[1,2,3], Chongyang Han[1,2,3], Stephen G Waxman[1,2,3], and Sulayman D Dib-Hajj[1,2,3]

Abstract

Sodium channels play pivotal roles in health and diseases due to their ability to control cellular excitability. The pore-forming α-subunits (sodium channel alpha subunits) of the voltage-sensitive channels (i.e., $Na_v1.1$–1.9) and the nonvoltage-dependent channel (i.e., Na_x) share a common structural motif and selectivity for sodium ions. We hypothesized that the actin-based nonmuscle myosin II motor proteins, nonmuscle myosin heavy chain-IIA/myh9, and nonmuscle myosin heavy chain-IIB/myh10 might interact with sodium channel alpha subunits to play an important role in their transport, trafficking, and/or function. Immunochemical and electrophysiological assays were conducted using rodent nervous (brain and dorsal root ganglia) tissues and ND7/23 cells coexpressing Na_v subunits and recombinant myosins. Immunoprecipitation of myh9 and myh10 from rodent brain tissues led to the coimmunoprecipitation of Na_x, $Na_v1.2$, and $Na_v1.3$ subunits, but not $Na_v1.1$ and $Na_v1.6$ subunits, expressed there. Similarly, immunoprecipitation of myh9 and myh10 from rodent dorsal root ganglia tissues led to the coimmunoprecipitation of $Na_v1.7$ and $Na_v1.8$ subunits, but not $Na_v1.9$ subunits, expressed there. The functional implication of one of these interactions was assessed by coexpressing myh10 along with $Na_v1.8$ subunits in ND7/23 cells. Myh10 overexpression led to three-fold increase ($P < 0.01$) in the current density of $Na_v1.8$ channels expressed in ND7/23 cells. Myh10 coexpression also hyperpolarized voltage-dependent activation and steady-state fast inactivation of $Na_v1.8$ channels. In addition, coexpression of myh10 reduced ($P < 0.01$) the offset of fast inactivation and the amplitude of the ramp currents of $Na_v1.8$ channels. These results indicate that nonmuscle myosin heavy chain-IIs interact with sodium channel alpha subunits subunits in an isoform-dependent manner and influence their functional properties.

Keywords

Myosins, nonmuscle myosin heavy chains, myh9, myh10, sodium channel, voltage clamp

Date Received: 10 March 2018; revised: 10 May 2018; accepted: 5 June 2018

Introduction

Sodium channels are integral membrane proteins found in the cells of all higher eukaryotes. They are made up of both alpha (α) and beta (β) subunits. Nine sodium channel alpha subunits (Na_α) are voltage gated (i.e., $Na_v\alpha$: $Na_v1.1$, $Na_v1.2$, $Na_v1.3$, $Na_v1.4$, $Na_v1.5$, $Na_v1.6$, $Na_v1.7$, $Na_v1.8$, and $Na_v1.9$), and only one Na_α subunit (i.e., Na_x) is gated by cellular sodium gradient.[1] $Na_v\alpha$ subunits are functional on their own, but they tend to associate with four known β subunits (i.e., $Na_v\beta1$, $Na_v\beta2$, $Na_v\beta3$, and $Na_v\beta4$), which are not functional on their own, to modulate their own functional properties.[2] $Na_v\alpha$ subunits mostly occur at central nervous system neurons (i.e., $Na_v1.1$, $Na_v1.2$, $Na_v1.3$, and $Na_v1.6$), skeletal muscles (SKMs) (i.e., $Na_v1.4$), uninnervated SKM (i.e., $Na_v1.5$), heart (i.e., $Na_v1.5$), parasymphathetic nervous system neurons (i.e., $Na_v1.7$), dorsal root ganglion (DRG) neurons (i.e., $Na_v1.7$, $Na_v1.8$, and $Na_v1.9$), astrocytes (i.e., Na_x), hypothalamus (Na_x), and so on.[1]

[1]Department of Neurology, Yale University School of Medicine, New Haven, CT, USA
[2]Center for Neuroscience and Regeneration Research, Yale University School of Medicine, New Haven, CT, USA
[3]Rehabilitation Research Center, VA Connecticut Healthcare System, West Haven, CT, USA

Corresponding Author:
Sulayman D Dib-Hajj, Neuroscience and Regeneration Research Center, VA Connecticut Healthcare System, 950 Campbell Avenue, Bldg. 34, West Haven, CT 06516, USA.
Email: sulayman.dib-hajj@yale.edu

Voltage-gated sodium channels (Na_vs) utilize cellular membrane potential to function, influx extracellular sodium into the cells, and fire action potentials in excitable cells such as neurons and myocytes (skeletal and cardiac).

The mechanisms by which neuronal Na_α subunits are trafficked to the cell surface are not well understood though considerable knowledge has been garnered over the years regarding their clustering at the axon initial segment and the nodes of Ranvier.[3–6] Generally, vesicles carrying membrane proteins traffic from the intracellular pools to the plasma membranes. This involves their transport by kinesin family of motor proteins (KIF) along the microtubules and/or by myosin family of motor proteins (myo or myh) along the actin filaments. Kinesin heavy chain-1 (KIF5B) has been shown to be involved in the trafficking of $Na_v1.2$[7] and $Na_v1.8$[8] subunits. Myosin Va (myoVa) is also shown to be involved in the trafficking of $Na_v1.2$ subunits.[9]

In recent years, class II nonmuscle myosins (i.e., NM-IIs) are shown to interact with various membrane proteins including chemokine receptor CXCR4 (in T lymphocytes),[10] epidermal growth factor receptor (EGFR),[11] N-methyl-d-aspartate receptor (NMDAR),[12] α-amino-3-hydroxy-5-methyl-4-isoxazole-propionic acid receptor (AMPAR),[13] the pore-forming subunit of P/Q-type calcium channels ($Ca_v2.1$),[14] a lysosomal membrane protein (Cln3),[15] Kv2.1 channels,[16] and so on. Class II NM-IIs, like class II muscle myosins (i.e., myh1, myh2, myh3, etc.), are hexameric molecules comprising two NM-II heavy chains (i.e., NMHC-IIA/myh9, NMHC-IIB/myh10, or NMHC-IIC/myh14), two myosin essential light chains (ELCs), and two myosin regulatory light chains (MRLCs).[17,18] The heavy chain comprises a globular head domain (the site for interaction with actin and ATP), a neck region (site for interaction with ELC and MRLC), and a tail region which homodimerizes in a helical fashion and is a possible site for interaction with the cargo.[17,18] NM-IIs interact only transiently with actin and typically spend most of their kinetic cycle detached from actin.[19] In contrast, myosin V moves processively along actin filaments and associates strongly with actin in the presence of ATP. These characteristics enable myoVa to function as an intracellular cargo motor.[19] Because of their known association with multiple classes of membrane proteins including ion channels, we hypothesized that NM-IIs might play an important role in the trafficking of Na_α subunits expressed in the neuronal tissues. Our results indicate that two NM-II isoforms, myh9 and myh10, interact with sodium channel subunits expressed in nervous tissues in an isoform-specific manner. We also show that the functional properties of $Na_v1.8$ channels are modulated by myh10. Hence, there appear to exist multiple pathways for trafficking of Na_α subunits to the cell membrane by two independent cellular motor proteins, myosins and kinesins.

Materials and methods

Plasmids

Green fluorescent protein (GFP) tagged NMHC II-B (i.e., myh10; National Center for Biotechnology Information reference: NM_005964/NP_005955; full length: 1976 amino acids) and AnkG270-mCherry were obtained from Addgene.[20,21] These constructs were subcloned or modified as needed. All other constructs were available in our laboratory. The $Na_v1.6$ construct harbors a mutation (Tyr371Ser) that renders it resistant to tetrodotoxin (TTX).

Cell culture and transfection

Human embryonic 293 cells (HEK293 cells), ND7/23 cells, and Nav1.6-GFP stable cell lines in HEK293 background were cultured according to standard procedures. Optifect (Thermo Fisher Scientific, Waltham, MA) or LipoJet (SignaGen Laboratories, Rockville, MD) transfection reagents were used according to manufacturer's instructions for transient transfections. ND7/23 cells (i.e., a hybrid of mouse neuroblastoma and rat DRG neurone) endogenously express $Na_v1.3$, $Na_v1.6$, and $Na_v1.7$ subunits and are considered as a model neuronal cell line for functional expression Na_v subunits.[22–25]

Antibodies

Various immunoglobulin (IgG) isotypes, mouse monoclonal antibodies, and rabbit polyclonal antibodies used for immunoprecipitation (IP), and/or immunoblot (IB) assays are provided in as Supplemental Tables (Tables S1 and S2). Antibody dilutions and/or concentrations used for IP and/or IB assays along with the molecular weight (~kDa) of the antigens detected by these antibodies are also provided (Table S2).

Immunoblots were incubated with monoclonal antibodies against myh9 (1:500; Abcam), myh10 (1:1000; Abcam), MRLC (1:200; Santa Cruz Biotechnology), Na_v subunits (pan-$Na_v\alpha$; 1:1000; Sigma), $Na_v1.1$ (1:500; NeuroMab), ankyrin-G (AnkG) (1:500; NeuroMab), ankyrin-B (1:500; NeuroMab), ankyrin-R (AnkR) (1 μg/mL; Santa Cruz Biotechnology), β-I spectrin (1:100; Abcam), α-II spectrin (1:500; Abcam), β-IV spectrin (1:500; NeuroMab), and β-actin (1:10,000; Sigma).

Polyclonal antibodies against $Na_v1.2$ (1:200; Alomone), $Na_v1.3$ (1:200; Alomone), $Na_v1.6$ (PN4; 1:200; Sigma), $Na_v1.7$ (1:200; Alomone), $Na_v1.8$ (1:200; Alomone), $Na_v1.9$ (1:200; Alomone), Na_x (1:1000; Abcam), β-II spectrin (1:2000; Abcam), β-III spectrin

(1 µg/mL; Santa Cruz Biotechnology), and GFP (1:1000; Invitrogen) were also used for immunoblotting.

The MRLC antibody (sc-28329; clone E4; Santa Cruz Biotechnology) is already shown to detect various MRLCs and hence considered as a pan-MRLC in some quarters.[26] It is claimed to recognize the MRLCs from human (i.e., MRCL3, MRLC2, MYL9, and LOC391722: MRLC 12B-like), mouse (i.e., Mylc2b, Myl9, and Myl12a), and rat (i.e., Mrlcb and Myl9) tissues. In our hand, it poorly detects the MRLCs from cell lysates, but it detects the MRLCs as a coimmunoprecipitate from precipitation of NMHC-IIs very well (Figures 1 to 3).

The aggregate pan-Na_v channel co-IP signals would not reflect any contribution from the Na_x subunit, as the pan-Na_v antibody (Sigma: Clone K58/35) is raised against an 18 amino acids epitope that is present only in the intracellular III to IV loop (i.e., TEEQKKYYNAMKKLGSKK) of the Na_v subunits.

Preparation of cell and tissue lysates or membrane fractions

All animal care and experimental studies were approved by the Veterans Administration Connecticut Healthcare System Institutional Animal Care and Use Committee. We followed the protocols published elsewhere with some modifications to prepare adult rat (Sprague-Dawley), postnatal day 3 rat (Sprague-Dawley), adult mouse (C57/BL6), and *Scn8a*^{medtg} mouse (i.e., $Na_v1.6$ null homozygous; postnatal day 12–14) brain or DRG tissue lysates for IP and immunoblotting.[7] This is because $Na_v1.3$ proteins are relatively better expressed in embryonic and neonatal brains. We also used young animal's brains as $Na_v1.6$ knockout (KO; *Scn8a*^{medtg}) mouse only survives up to two to three weeks after birth. Adult rodents were used for all other applications because they provide larger starting material for the biochemical assays, thus allowing us to reduce the number of animals used in these studies.

The lysis or IP buffer was made of 20 mM Tris-Cl (pH 7.4), 150 mM NaCl, 1% Triton X-100, 1 mM DTT, 10 mM EGTA, and 2× complete protease inhibitor cocktail (Roche Diagnostics Corporation, Indianapolis, IN). A whole animal (male or female) brain was homogenized in pieces in a tissue grinder (Qiagen, Valencia, CA) to a final volume of ~50 mL lysis buffer. Homogenates were solubilized for 2 h at 4°C and centrifuged at 50,000 g for 30 min at 4°C using a Beckman Coulter Optima® ultracentrifuge to collect the

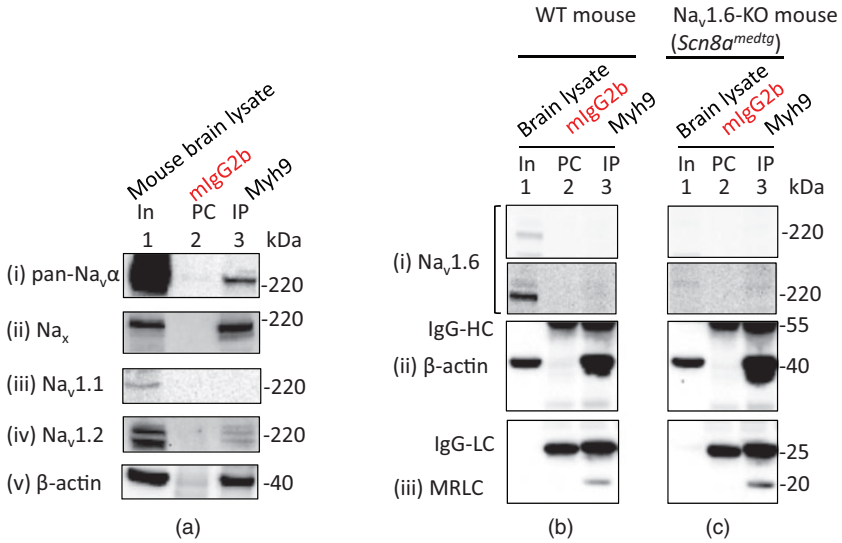

Figure 1. Interaction of myh9 with Na_x subunits expressed in the mouse brain tissues. WT type (In, lane 1 in (a) and (b)) or $Na_v1.6$ KO (*Scn8a*^{medtg}; In, lane 1 in (c)) mouse brain tissue lysates were PC with mouse IgG2b isotypes (PC, lane 2 in (a), (b), and (c)) prior to IP using mouse anti-myh9 antibodies (IP, lane 3 in (a), (b), and (c)) of the IgG2b isotypes. Myh9 coimmunoprecipitated pan-Na_v ((i) in (a)), Na_x ((ii) in (a)), and $Na_v1.2$ ((iv) in (a)) subunits, but not $Na_v1.1$ subunits ((iii) in (a)), expressed in mouse brain tissues. $Na_v1.6$ subunits ((i) in (b)) were not coimmunoprecipitated with myh9 expressed in the mouse brain tissues. As expected, there was not any $Na_v1.6$ immunoreactivity from *Scn8a*^{medtg} mouse brain tissues ((i) in (c)). Myh9 also coimmunoprecipitated β-actin ((v) in (a) and (ii) in (b) and (c)) and MRLCs ((iii) in (b) and (c)) expressed in mouse brain tissues. The MRLC immunoreactive signal from the mouse brain tissue lysates is barely detectable. Mouse IgG-HC (panel (ii) in (b) and (c)) and IgG-LC (panel (iii) in (b) and (c)), which are separated from their intact immunoglobulins (i.e., used for PC or IP) upon denaturation, could be seen as these blot sections are probed with mouse (anti-β-actin and anti-MRLC) antibodies. Additional information is available in Figure S1. IgG-LC: immunoglobulin light chain; IgG-HC; immunoglobulin heavy chain; In: lysate input; IP: immunoprecipitation; KO: knockout; mIgG2b: mouse immunoglobulin isotype 2b; MRLC: myosin regulatory light chain; myh: myosin heavy chain; Na_v: voltage-sensitive sodium channel; Na_x: nonvoltage-dependent sodium channel; PC: precleared; WT: wild type.

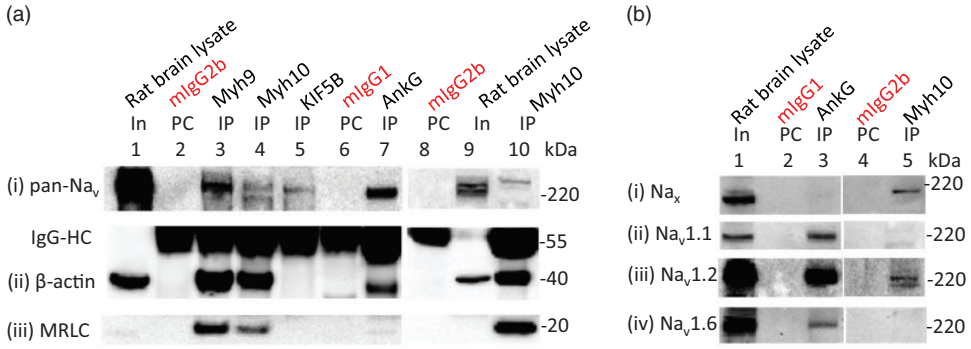

Figure 2. Interaction of myh9 and myh10 with Na_v subunits expressed in the rat brain tissues. (a) Myh9 and myh10 interact with pan-Na_v subunits expressed in the rat brain tissues. Rat brain tissue lysates (In, lanes 1 and 9) were PC with mouse IgG2b isotypes (PC, lanes 2 and 8) and mouse IgG1 isotypes (PC, lane 6) prior to IP using indicated antibodies (lane 3 = myh9, lanes 4 and 10 = myh10, lane 5 = KIF5B, and lane 7 = AnkG) of the same isotypes as those were used for preclearing. IP complexes in the gel were loaded following the loading of their respective isotype (PC) complexes. Pan-Na_v subunits (i) were coimmunoprecipitated with myh9, myh10, KIF5B, and AnkG expressed in the rat brain tissues. CoIP of pan-Na_v subunits by AnkG and KIF5B served as positive controls. Myh9 and myh10 coimmunoprecipitated β-actin (ii) and MRLCs (iii) expressed in the rat brain tissues. Anti-MRLC antibodies poorly detect their antigens from rat brain tissue lysates (lane 1 in (iii)). AnkG also coimmunoprecipitated β-actin and MRLCs expressed in the rat brain tissues. Denatured mouse IgG-HC (iii) separated from their intact immunoglobulins (i.e., used for PC or IP) could be seen in the immunoblot, as this section of the blot was probed with mouse anti-β-actin antibodies. (b) Interaction of myh10 with Na_α subunits expressed in the adult rat brains. Rat brain tissue lysates (In, lane 1) were PC with mouse IgG1 isotypes (PC, lane 2) and mouse IgG2b isotypes (PC, lane 4) prior to IP using antibodies for AnkG (IP, lane 3) and myh10 (IP, lane 5) of the of the same isotypes as those were used for preclearing. Loading of isotype (PC) complexes in the gel preceded those of the IP complexes. Myh10 coimmunoprecipitated Na_x (i) and $Na_v1.2$ (iii) subunits, but not $Na_v1.1$ (ii) and $Na_v1.6$ (iv) subunits, from rat brain tissues. As expected, AnkG coimmunoprecipitated $Na_v1.1$ (ii), $Na_v1.2$ (iii), and $Na_v1.6$ (iv) subunits, but not Na_x (i) subunits, expressed in rat brain tissues. AnkG: ankyrin-G; IgG-HC: immunoglobulin heavy chain; In: lysate input; IP: immunoprecipitation; KIF5B: kinesin family member 5B; mIgG1: mouse immunoglobulin isotype 1; mIgG2b: mouse immunoglobulin isotype 2b; MRLC: myosin regulatory light chain; myh: myosin heavy chain; Na_v: voltage-sensitive sodium channel; Na_x: nonvoltage-dependent sodium channel; PC: precleared.

supernatants for IP and immunoblotting. The rat DRG lysates were prepared in the similar manner except that the largest DRG pairs (three pairs: L4–L6) from an adult rat (male or female) was homogenized to a final volume of 1 mL lysis buffer. Nontransfected HEK293 cells (control), cells transiently transfected with plasmid constructs, and $Na_v1.6$-GFP cells were collected by centrifugation at 500 g for 5 min at 4°C upon trypsinization. These pellets were washed twice with ice-cold phosphate-buffered saline by centrifugation at 500 g for 5 min at 4°C before lysis using the IP buffer. Cell supernatants were obtained by centrifugation at 15,000 g for 20 min at 4°C for IP and immunoblotting.

Solubilized mouse brain membrane fractions for antibody characterization (Figure S2) were prepared according to the protocol reported elsewhere.[27] Protein concentrations in the tissue lysates and membrane preparations were determined using the Bradford reagent (Bio-Rad, Hercules, CA).

Immunoprecipitation

For IP experiment, HEK293 cell or animal tissue supernatants containing 0.5 to 4 mg protein (in ~1 mL lysate) was precleared (PC) for 1 to 4 h at 4°C with 5 to 10 µg of suitable mouse antibody isotypes or rabbit IgG and 80 to 100 µL of Dynabead® protein G (Thermo Fisher Scientific). PC supernatants were incubated (overnight, 4°C) with 5 to 10 µg of desired IP antibody (Table S1) and 80 to 100 µL of Dynabead® protein G. Dynabead® protein G beads bound to control antibody isotypes (i.e., PC complexes) or desired primary antibodies (i.e., IP complexes) were washed for five times with IP buffer or wash buffer supplied by the vendor (Thermo Fisher Scientific) and eluted with NuPAGE® LDS Sample Buffer (Thermo Fisher Scientific) in the presence of NuPAGE® Sample Reducing Agent (Thermo Fisher Scientific).

Western blotting

About 20 to 50 µg of HEK293 cell or animal tissue lysates were denatured using NuPAGE® Sample Reducing Agent in the presence of NuPAGE® LDS Sample Buffer to serve as input (In) sample for Western blotting. The input samples, PC complexes, IP complexes, and/or at times denatured depleted supernatants were resolved on NuPAGE® Novex® 4% to 12% Bis-Tris Gels (1.0 mm, 12 well) and transferred to a nitrocellulose membrane. Membranes were blocked

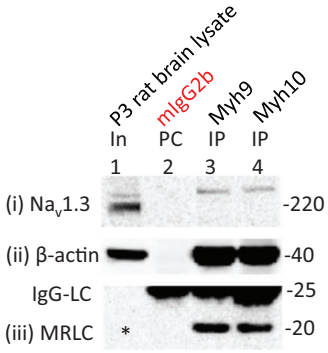

Figure 3. Interaction of myh9 and myh10 with $Na_v1.3$ subunits expressed in the postnatal day 3 (P3) rat brain tissues. P3 rat brain tissue lysates (In, lane 1) were PC with mouse IgG2b isotypes (PC, lane 2) prior to IP using mouse anti-myh9 (IP, lane 3) and mouse anti-myh10 (IP, lane 4) antibodies of the IgG2b isotypes. Loading of mIgG2b (PC) complexes in the gel preceded those of the IP complexes. Myh9 and myh10 coimmunoprecipitated $Na_v1.3$ subunits (i) expressed in P3 rat brain tissues. Myh9 and myh10 also coimmunoprecipitated β-actin (ii) and MRLCs (iii) expressed in P3 rat brain tissues. The MRLC immunoreactive signal from the rat tissue lysates is barely detectable and is indicated with an asterisk (*). The denatured mouse IgG-LC (iii) separated from their intact immunoglobulins (i.e., used for PC or IP) could be seen in the immunoblot, as this section of the blot is probed with mouse anti-MRLC antibodies. IgG-LC: immunoglobulin light chain; In: lysate input; IP: immunoprecipitation; mIgG2b: mouse immunoglobulin isotype 2b; MRLC: myosin regulatory light chain; myh: myosin heavy chain; Na_v: voltage-sensitive sodium channel; PC: precleared.

using a blocking buffer (5% nonfat dry milk and 1% bovine serum albumin (BSA) in 0.1% tris-buffered saline with Tween 20 (TBST) or 5% BSA in 0.1% TBST) for 1 h, washed, and incubated overnight with desired primary antibodies (Table S2) diluted in the blocking buffer. The blots were washed and incubated in horseradish peroxidase-conjugated goat antimouse (1:10,000; Dako, Santa Clara, CA) or goat antirabbit (1:10,000; Dako, Santa Clara, CA) for 1 h. The blots were washed extensively and developed for 1 to 10 min with the Perkin Elmer Western Lightning Plus-enhanced chemiluminescence kit using a Bio-Rad ChemiDoc XRS+ or ChemiDoc Imaging System. At times, IBs were stripped using a stripping buffer (Thermo Fisher Scientific) to reprobe with another primary antibody. We usually cut through the IgG-heavy chain (HC) and/or IgG-light chain (LC) regions of the Ponceau S (Sigma) stained nitrocellulose membranes for probing different section of the membrane with different antibodies. Therefore, cut marks could be seen across the IgG-HC and/IgG-LC immunoreactive bands.

Voltage-clamp analysis

ND7/23 cells were cultured on 12-mm glass coverslips coated with poly-D-lysine/laminin (BD Biosciences, San Jose, CA) and transfected with $Na_v1.8$ cDNA and GFP-myh10 (or GFP control) using Lipofectamine 2000 (Invitrogen, Carlsbad, CA). After 48 h, cells with robust green fluorescence were selected for recording. Whole-cell voltage-clamp recordings of ND7/23 cells were performed at room temperature (20°C–22°C) using an EPC-9 amplifier (HEKA Electronics, Lambrecht/Pfalz, Germany). Fire-polished electrodes (0.6–1.5 MΩ) were fabricated from 1.6 mm outer diameter borosilicate glass micropipettes (World Precision Instruments, Sarasota, FL). The pipette potential was adjusted to zero before seal formation, and liquid junction potential was not corrected. Capacity transients were cancelled, and voltage errors were minimized with 80% to 90% series resistance compensation. Currents were acquired with Pulse Software (HEKA Electronics), 5 min after establishing whole-cell configuration, sampled at a rate of 50 kHz, and filtered at 2.9 kHz. For current–voltage relationships, cells were held at −80 mV and stepped to a range of potentials (−60 to +50 mV in 5 mV increments) for 100 ms. Peak inward currents (I) were plotted as a function of depolarization potential to generate I–V curves. Activation curves were obtained by converting I to conductance (G) at each voltage (V) using the equation $G = I/(V - V_{rev})$, where V_{rev} is the reversal potential which was determined for each cell individually. Activation curves were then fit with Boltzmann functions in the form of $G = G_{max}/\{1 + \exp[(V_{1/2,act} - V)/k]\}$, where G_{max} is the maximal sodium conductance, $V_{1/2,act}$ is the potential at which activation is half maximal, V is the test potential, and k is the slope factor. Steady-state fast inactivation was achieved with a series of 500-ms prepulses (−90 to 10 mV in 5 mV increments), and the remaining noninactivated channels were activated by a 40-ms step depolarization to 10 mV. Peak inward currents obtained from steady-state fast inactivation protocols were normalized to the maximal peak current (I_{max}) and fit with Boltzman functions: $I = A + (1 - A)/(1 + \exp[(V_m - V_{1/2,inact})/k])$, where V_m represents the inactivating prepulse membrane potential, and $V_{1/2,inact}$ represents the midpoint of inactivation. Ramp currents were elicited with a slow depolarizing voltage ramp from −80 to 40mV at a rate of 0.2 mV/ms. The absolute ramp current amplitude was normalized to the maximal peak current obtained by I–V protocol. The pipette solution contained (in mM) 140 CsF, 10 NaCl, 1 EGTA, and 10 HEPES, pH 7.30 (adjusted with CsOH). Osmolarity was adjusted to 310 mOsmol/L with dextrose. The extracellular bath solution contained (in mM) 140 NaCl, 3 KCl, 1 $MgCl_2$, 1 $CaCl_2$, 10 HEPES, 5 CsCl, and 20 tetraethylammonium chloride, pH 7.3 with NaOH (327 mOsmol/L). TTX (500 nM) was added to the bath solution to block the endogenous TTX-sensitive voltage-gated sodium currents from ND7/23 cells.

Data analysis

Data were analyzed using FitMaster (HEKA Electronics) and Origin 8.5 professional (Microcal Software, Northampton, MA) and presented as means ± standard error of the mean. Except where noted, statistical significance was determined by unpaired Student's *t* tests.

Results

Interaction of myh9 with Na_α subunits expressed in the mouse brain

We hypothesized that NM-IIs might interact with the Na_α subunits. One of the specific hypotheses we tested was that NM-IIA (i.e., myh9) might interact with $Na_v1.6$ subunits expressed in the brain tissues. We tested this hypothesis using mouse brain tissues as a suitable control (i.e., *Scn8a*^{medtag}/$Na_v1.6$ KO mouse) was available to us. Results indicated a lack of interaction of myh9 with $Na_v1.6$ expressed in mouse brain tissues (Figure 1 (a) and (c); Figure S1). As expected, myh9 coimmunoprecipitates its partner proteins β-actin and MRLCs from both wild type and $Na_v1.6$ KO mouse tissues (Figure 1(b) and (c); Figure S1). These results did not indicate whether myh9 interacts with other Na_α subunits expressed in mouse brain tissues. As a first step, we immunoprecipitated myh9 from adult mouse brain tissues and probed for co-IP of pan-$Na_v\alpha$ subunits expressed there (Figure 1(a)). Co-IP of pan-Na_v subunits was observed with myh9 expressed in mouse brain tissues (Figure 1(a)). The pan-Na_v co-IP signal observed could be as a result of interaction of one or more Na_v isoforms (i.e., $Na_v1.1$, $Na_v1.2$, and/or $Na_v1.6$) with myh9 expressed in mouse brain tissues. Further analysis indicated that myh9 coimmunoprecipitate Na_x subunits, $Na_v1.2$ subunits, but not $Na_v1.1$ subunits, expressed in adult mouse brain tissues (Figure 1(a)). $Na_v1.2$ co-IP signals from mouse brain tissues (and also from rat brain tissues in Figure 2; see next section) revealed multiple immunoreactive bands possibly indicating that $Na_v1.2$ subunits exist in multiple modified states as a result of posttranslational modifications, degradation; and so on.[28]

Interaction of myh9 and myh10 with Na_α subunits expressed in the rat brain

We wanted to recapture the myh9 and Na_v interaction observed in the mouse brain tissues in rat brain tissues. We also wanted to know whether myh10, another nonmuscle myosin isoform, would interact with the same Na_v subunits those interact with myh9. To this end, both myh9 and myh10 were immunoprecipitated from adult rat brain tissues and probed for co-IP of pan-$Na_v\alpha$ subunits. (Figure 2(a)). We also immunoprecipitated AnkG and kinesin-1 heavy chain (i.e., KIF5B) to control for co-IP of pan-Na_v subunits, as they are known to interact with various Na_v subunits.[4,7,29,30] Results indicated co-IP of pan-Na_v subunits with both myh9 and myh10 expressed in rat brain tissues (Figure 2(a)). As expected, both myh9 and myh10, but not KIF5B, coimmunoprecipitated β-actin and MRLCs expressed in the rat brain tissues (Figure 2(a)). Both KIF5B and AnkG also coimmunoprecipitated pan-Na_v subunits from rat brain tissues (Figure 2(a)).

This AnkG antibody also pulled down β-actin from rodent brain tissues which could be attributed to its interaction with actin-binding proteins such as spectrins (Figure 2).[31] We also observed that AnkG coimmunoprecipitated MRLCs with (Figure 2) which could be as a result of direct interaction of AnkG with MRLCs or its interaction with proteins (e.g., myosins) which interact with MRLCs.[32–34] In addition, we show that IP of AnkG using the same antibody led to the IP of its cognate antigens (i.e., all the three isoforms of 480, 270, and 190 kDa) and co-IP of $Na_v1.1$ subunits, $Na_v1.2$ subunits, $Na_v1.6$ subunits, α-II spectrin, β-II spectrin, β-III spectrin, and β-IV spectrin (all known to interact with AnkG), but not βI-spectrin and the Na_x subunits (which are known not to partner with AnkG), expressed in rat brain tissues (Figure 2; Figure S3).[4,29,30]

The pan-Na_v immunoreactive co-IP signals indicate that one or more Na_v isoforms expressed in the adult rat brain tissues (i.e., $Na_v1.1$, $Na_v1.2$, and/or $Na_v1.6$) might be interacting with both of these myosins. Hence, we wanted to know which Na_v isoforms interact with NM-IIs expressed in the rat brain tissues. Results indicated co-IP of $Na_v1.2$ subunits but not $Na_v1.1$ and $Na_v1.6$ subunits with myh10 expressed in adult rat brain tissues (Figure 2(b)). Myh10 also coimmunoprecipitated the atypical sodium channel, Na_x, subunits expressed in rat brain tissues (Figure 2(b), (i)).

Then, we wanted to determine whether $Na_v1.3$ subunits expressed in rat brain tissues would interact with myh9 and/or myh10. To this end, we immunoprecipitated myh9 and myh10 from postnatal day 3 (P3) rat brain tissues, as these tissues are known to express $Na_v1.3$ subunits. IP of myh9 and myh10 from P3 rat brain tissues led to the co-IP of $Na_v1.3$ subunits expressed there (Figure 3).

Reciprocally, we wanted to know whether IP of pan-Na_v subunits from adult rat brain tissues would lead to co-IP of myh9 and/or myh10 expressed there (Figure S4). Pan-Na_v antibodies could not coimmunoprecipitate myh9 expressed in rat brain tissues. There appears to be some degree of co-IP of myh10 by pan-Na_v subunits expressed in rat brain tissues (Figure S4). As expected, pan-Na_v subunits coimmunoprecipitated AnkG (which

occurs as three different isoforms of 190, 270, and 480 kDa) and AnkR[5] from rat brain tissues (Figure S4).

Interaction of myh9 and myh10 with Na_v subunits expressed in the rat DRGs

$Na_v1.7$, $Na_v1.8$, and $Na_v1.9$ subunits are predominantly expressed in adult DRG tissues. Therefore, we wanted to determine whether any of these Na_v subunits expressed in the rat DRGs would coimmunoprecipitate with myh9 and myh10 expressed there.[35] We also immunoprecipitated KIF5B to control for co-IP of $Na_v1.8$ subunits as a positive interaction for the two proteins has been reported previously.[8] IP of myh9 and myh10 led to the co-IP of $Na_v1.7$ and $Na_v1.8$ subunits but not $Na_v1.9$ subunits expressed in rat DRGs (Figure 4(a)). As expected, KIF5B also coimmunoprecipitated $Na_v1.18$ subunits expressed in rat DRGs. These results also indicated that KIF5B do not interact with $Na_v1.7$ and $Na_v1.9$ subunits expressed in rat DRGs.

On a reciprocal basis, we wanted to know whether $Na_v1.7$ or $Na_v1.8$ subunits would coimmunoprecipitate myh9 and/or myh10 expressed in the DRGs (Figure 4 (b)). We immunoprecipitated $Na_v1.7$ and $Na_v1.8$ subunits from rat DRG tissues using antibodies already reported suitable for such reactions.[36–38] $Na_v1.7$ subunits coimmunoprecipitated myh9 and myh10 from rat DRGs (Figure 4(b)). Also, myh9 and myh10 were coimmunoprecipitated with $Na_v1.8$ subunits expressed in rat DRGs (Figure 4(b)).

Functional effects of myh10 overexpression on the electrophysiological properties of $Na_v1.8$ channels heterologously expressed in ND7/23 cells

Earlier we demonstrated that both myh9 and myh10 interact with $Na_v1.8$ subunits. We investigated whether such interaction would influence the electrophysiological properties of $Na_v1.8$ channels. To this end, we coexpressed human $Na_v1.8$ subunits along with GFP (Figure 5(a)) or GFP-myh10 (Figure 5(b)) in ND7/23 cells. Representative $Na_v1.8$ sodium channel currents recorded from cells expressing GFP or myo10-GFP in the presence of $Na_v1.8$ subunits are shown in Figure 5(a)

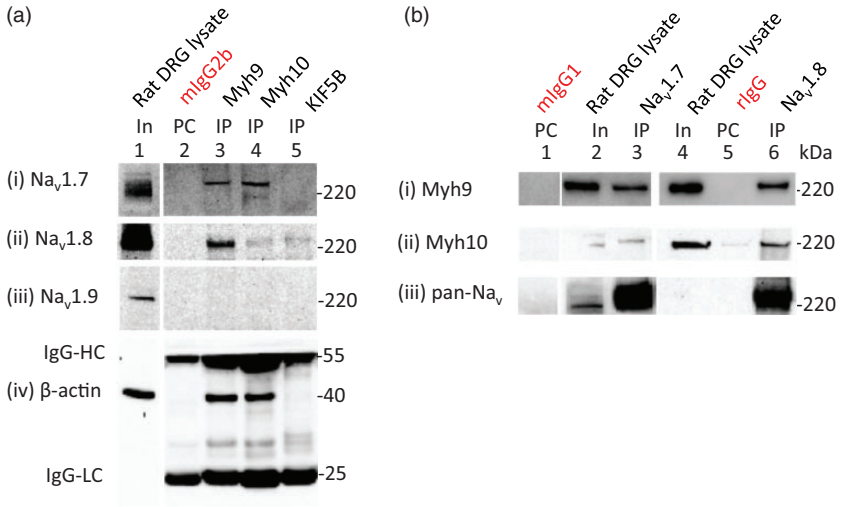

Figure 4. Interaction of myh9 and myh10 with Na_v subunits expressed in adult rat DRG tissues. (a) Interaction of myh9 and myh10 with Na_v subunits expressed in adult rat DRG tissues. Adult rat DRG tissue lysates (In, lane 1) were PC with mouse IgG2b isotypes (PC, lane 2) prior to IP using mouse anti-myh9 (IP, lane 3), anti-myh10 (IP, lane 4), and anti-KIF5B antibodies of IgG2b isotypes. Loading of IgG2b (PC) complexes in the gel preceded those of the IP complexes. Myh9 and myh10 coimmunoprecipitated $Na_v1.7$ (i) and $Na_v1.8$ (ii) subunits, but not $Na_v1.9$ (iii) subunits, expressed in rat DRG tissues. As expected, both myh9 and myh10, but not KIF5B, coimmunoprecipitated β-actin expressed in rat DRG tissues. KIF5B also coimmunoprecipitated $Na_v1.8$ subunits, but not $Na_v1.7$ and $Na_v1.9$ subunits, expressed in rat DRG tissues. Mouse IgG-HC (iv) and IgG-LC (iv), which are separated from their intact immunoglobulins upon denaturation, are seen, as this blot section was probed with mouse (anti-β-actin) antibodies. (b) Interaction of $Na_v1.7$ and $Na_v1.8$ subunits with myh9 and myh10 expressed in adult rat DRG tissues. Adult rat DRG tissue lysates (In, lanes 2 and 4) were PC with mouse IgG1 isotypes (PC, lane 1) and rabbit IgG (PC, lane 5) prior to IP using mouse anti-$Na_v1.7$ (IP, lane 3) antibodies of IgG1 isotypes and rabbit anti-$Na_v1.8$ (IP, lane 6) antibodies. Loading of PC complexes in the gel preceded those of the IP complexes. $Na_v1.7$ and $Na_v1.8$ subunits coimmunoprecipitated myh9 (i) and myh10 (ii) expressed in rat DRG tissues. Probing with pan-Na_v antibodies revealed the IP signals for $Na_v1.7$ and $Na_v1.8$ subunits (iii). An asterisk (*) indicates loss of input signals following stripping the blot to probe for $Na_v1.8$ IP signals using pan-Na_v antibodies. DRG: dorsal root ganglia; IgG-HC: immunoglobulin heavy chain; In: lysate input; IP: immunoprecipitation; KIF5B: kinesin family member 5B; mIgG1: mouse immunoglobulin isotype 1; mIgG2b: mouse immunoglobulin isotype 2b; myh: myosin heavy chain; Na_v: voltage-sensitive sodium channel; PC: precleared; rIgG: rabbit immunoglobulins.

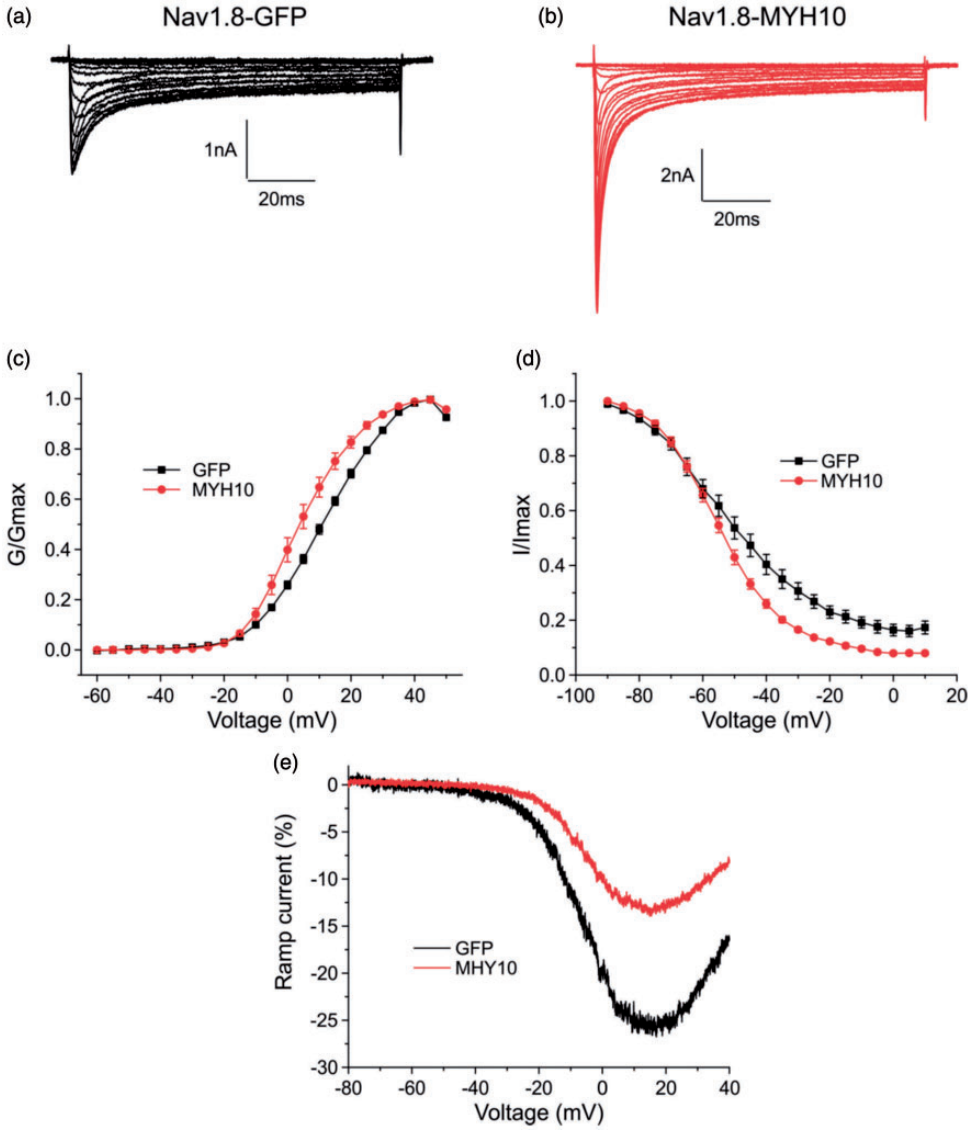

Figure 5. Coexpression of myh10 increases peak current density of $Na_v1.8$ channels heterologously expressed in ND7/23 cells. Representative sodium currents were recorded from ND7/23 cells transiently expressing $Na_v1.8$ in the presence of GFP (a) or GFP-myh10 (b). Cells were held at −80 mV, and sodium currents were elicited by a series of step depolarizations from −60 to +50 mV in 5-mV increments. (c) Coexpression of myh10 hyperpolarized activation of $Na_v1.8$. (d) Coexpression of myh10 enhanced steady-state fast inactivation of $Na_v1.8$. (e) Coexpression of myh10 reduced the amplitude of the ramp currents. GFP: green fluorescent protein; myh: myosin heavy chain.

and (b), respectively. Myh10 significantly increased the current density of $Na_v1.8$ channel by three-fold (GFP control: 50.9 ± 10.3 pA/Pf, $n = 17$; myh10: 135 ± 26 pA/pF, $n = 16$, $P < 0.01$). To examine the voltage dependence of activation, cells were held at −80 mV and stepped to a range of potentials (−60 to +50 mV in 5 mV increments) for 100 ms. As shown in Figure 5(c), myh10 coexpression hyperpolarized voltage-dependent activation of $Na_v1.8$ channels. When fitted with Boltzmann plots, the midpoint of activation was significantly more negative for myh10 (4.8 ± 1.6 mV, $n = 11$) than for GFP control (10.9 ± 0.7 mV, $P < 0.01$; $n = 13$), a shift of −6.1 mV in the hyperpolarizing direction. The slope for the activation curve for the myh10 condition (8.1 ± 0.3, $n = 11$) was also significantly different from that for the GFP control (9.6 ± 0.2, $n = 13$, $P < 0.001$). Myh10 also affected the steady-state fast inactivation of $Na_v1.8$ channels (Figure 5(d)). Myh10 hyperpolarized the fast inactivation curve. Although the middle point of fast inactivation for myh10 condition (-54.7 ± 1.2 mV, $n = 9$) was not significantly different from that of the GFP control (-51.7 ± 2.1 mV, $n = 10$),

the slope for the myh10 condition (9.3 ± 0.2, $n = 9$) was significantly smaller than that for the GFP control (12.3 ± 0.6, $n = 10$, $P < 0.001$). In addition, coexpression of myh10 reduced the offset of fast inactivation (GFP control: $16.2 \pm 2.0\%$, $n = 10$; myo10: 8.9 ± 0.8, $n = 9$, $P < 0.01$). We also investigated the effect of myh10 on $Na_v1.8$ ramp currents. As shown in Figure 5(e), myh10 significantly reduced the amplitude of the ramp currents ($14.1 \pm 0.6\%$, $n = 10$, $P < 0.01$) compared with the GFP control ($25.4 \pm 2.4\%$, $n = 9$).

Discussion

Class II myosins, with 15 members (i.e., myh1, myh2, myh3, myh4, myh6, myh7, myh7b, myh8, myh9, myh10, myh11, myh13, myh14, myh15, and myh16) in this group, are the largest class of myosins in vertebrates and are traditionally known as "conventional myosins." Most of these class II myosins are expressed in muscle (skeletal, smooth, and/or cardiac) cells. However, myh9, myh10, and myh14 are expressed widely in nonmuscle myosins and are known as nonmuscle class II myosin (NM-IIs or NMHC-IIs). Myh10 is more abundant than any other NM-IIs in neuronal tissues and thus has garnered much attention to for its role in brain structure and function.[13,39–41] In this work, we show that both myh9 and myh10 interact with Na_x, $Na_v1.2$, $Na_v1.3$, $Na_v1.7$, and $Na_v1.8$ subunits expressed in the nervous tissues. Interaction of myh9 with Na_x, $Na_v1.2$, $Na_v1.3$, $Na_v1.7$, and $Na_v1.8$ subunits led to the discovery of their interaction with myh10. This was anticipated because both myh10 and myh9 are homologous protein molecules possibly possessing some of the same structural and functional features for their interaction with Na_α subunits, although they are engaged in unique and diverse functions.[13,41–43] For the same reason, we also anticipated that a lack of interaction of $Na_v1.1$, $Na_v1.6$, or $Na_v1.9$ subunits with myh9 would lead to a similar outcome involving myh10. We could not assess the interaction Na_α subunits with myh14, the third member of the NM-II group, due to lack of suitable antibodies for its IP. The interaction of myh9 and myh10 with only a subset of channel isoforms increases confidence that these interactions are specific and not an artifact of the biochemical assay.

In general, in some of the IBs, the pan-Na_v and Na_v subunit-specific immunoreactive bands appear different in the input and/or IP lanes. Several factors could contribute to these observations including the amount of total and target proteins in the sample. It could be seen that the recombinant $Na_v1.6$ (detected by three different antibodies in lanes 3, 6, and 9) appears to run evenly and homogenously compared to Na_vs detected from native tissues (Figure S2). This could be due to the fact that native Na_vs are known to be heavily glycosylated and at least two additional isoforms, $Na_v1.1$ and $Na_v1.2$, are present in brain tissues. It is also possible that posttranslational modifications of Na_vs might occur in varying degrees in different tissue types (native tissues vs. HEK293 cells) which might contribute to their different mobilities on the IBs.[44,45]

The interaction of NM-IIs with Na_vs is consistent with previous observations that NM-IIs associate with membrane proteins and regulate their trafficking and/or function. For example, myh9 is associated with the trafficking and/or function of chemokine receptor CXCR4 (in T lymphocytes)[10] and EGFR.[11] Similarly, myh10 is associated with the trafficking and/or function of two members of the ionotropic glutamate receptors (i.e., NMDAR[12] and AMPAR[13]), $Ca_v2.1$ (the pore-forming subunit of P/Q-type calcium channels),[14] Cln3 (juvenile Batten disease protein/battenin/formerly known as juvenile neuronal ceroid lipofuscinosis: a lysosomal membrane protein),[15] and so on. A recent report also implicates NM-II in the sorting and post-Golgi dendritic trafficking of Kv2.1 channels.[16] Based on these results, we hypothesize that both myh9 and myh10 might be involved in the trafficking of the Na_α subunits with which they interact.

Most myosins, if not all, use adaptor or partner proteins to move or interact with their cargo.[11,46,47] Na_v subunits use various adaptor proteins such as AnkG,[48] AnkR,[5] syntrophin family of dystrophin-associated proteins,[49] 14-3-3,[50] plakophilin-2,[51] and so on, for their targeting, trafficking, membrane retention and organization, and regulation of their functional properties. It is possible that NM-IIs are also interacting with any of these or here-to-unknown adaptor proteins, thereby indirectly establishing contact with the Na_α subunits with which they interact (Figure 6). Hence, the formation of a myosin-adaptor-Na_α tripartite complex is plausible. This would be similar to the observation made recently that KIF5B uses AnkG as an adaptor to transport $Na_v1.2$ subunits.[7] Preliminary results from our work (*Soc. Neurosci. Abst.* (2016) 501.02/G39) also indicate that both myh9 and myh10 interact with AnkG giving credence to the idea that there possibly exist a myosin–ankyrin–Na_α pathway in neuronal and/or nonneuronal tissues (Figure 6). It appears that both myh9 and myh10 are using a common adaptor molecule (such as AnkG) to interact with some of the Na_v subunits (such as $Na_v1.2$ and $Na_v1.8$) and other unique or common adaptor molecules for their interaction with $Na_v1.3$, $Na_v1.7$, and Na_x subunits.

Our functional data show that coexpression of myh10 affects the current density and gating properties of the $Na_v1.8$ channels. Previous studies have not addressed whether NM-IIs would have any effect on the gating properties of the ion channels with which they interact.[12–14,16] In this study, the changes in current density

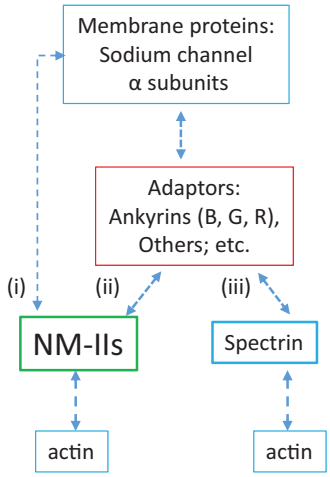

Figure 6. A model for interaction for NM-IIs with mammalian sodium channel α subunits. NM-IIs could be interacting with Na_α subunits directly (i) or via adaptor proteins (such as ankyrins) (ii). Also shown in the model the canonical spectrin–ankyrin–Na_v signaling network. NM-II: nonmuscle myosin II.

rather than the changes in gating properties of $Na_v1.8$ channels as a result myh10 overexpression may be its major contribution. The large (three-fold) increase in $Na_v1.8$ current density could be partly ascribed to an increase in number of functional ion channels on the cell surface as a result of myh10 overexpression. The effect of myh10 overexpression on the current density of $Na_v1.8$ might also be underestimated, as there is robust natural expression myh10 in ND7/23 cells These results are analogous to the observation that KIF5B increases the current density and surface expression of $Na_v1.8$ channels in both cultured DRG neurons and ND7/23 cells.[8] These authors[8] also concluded that a stretch of 10 amino acid sequence (i.e., from 511–620) in the stalk domain of KIF5B mediates its interaction with $Na_v1.8$ subunit (via its N-terminus). It is plausible that both myh9 and myh10 are using a conserved region or motif located away from their divergent and nonhomologous tail regions for their interaction with Na_α subunits. These data support the idea that interaction of NM-IIs with Na_v subunits could be functionally important.

Here, we provide evidence for the first time that class II nonmuscle myosins (myh9 and myh10) interact with a subset of Na_α (both Na_v and Na_x). Our data also show that the interaction of NM-IIs and Na_v subunits can be important for regulation of channel functions. Overall, our data support the conclusion that myh9 and myh10 interact specifically with a subset of sodium channels and suggest a model in which the actin–myosin network is involved in the regulation of function of sodium channels expressed in neurons, including DRG sensory neurons.

Author Contributions

BD conducted the biochemical experiments, analyzed the results, and wrote most of the paper. CH conducted the voltage clamp experiments and analyzed the results. BD, SDD-H, and SGW conceived the idea for the project and wrote the paper.

Acknowledgments

The authors thank Fadia Dib-Hajj and Palak Shah for molecular biology support. The authors also thank Shujun Liu, Peng Zhao, and Lawrence J Macala for providing animal tissues. Portions of this work were presented in two abstract forms: (1) Dash B, Han C, Akin EJ, Dib-Hajj SD and Waxman SG. Myosins interact with voltage gated sodium channels, sodium calcium exchangers and sodium potassium ATPases. *Soc Neurosci Abst* 2017; 288.11/D32 and (2) Dash B, Han C, Dib-Hajj F, Shah P, Waxman SG and Dib-Hajj SD. Ankyrin G is an anchor for myosins and voltage-gated sodium channels in the nervous system. *Soc Neurosci Abst* 2016; 501.02/G39.

Declaration of Conflicting Interests

The author(s) declared no potential conflicts of interest with respect to the research, authorship, and/or publication of this article.

Funding

The author(s) disclosed receipt of the following financial support for the research, authorship, and/or publication of this article: This work was supported in part by grants from the Rehabilitation Research Service and Medical Research Service, Department of Veterans Affairs (to SDD-H. and SGW). The Center for Neuroscience and Regeneration Research is a Collaboration of the Paralyzed Veterans of America with Yale University.

Supplemental Material

Supplementary material is available for this article Online.

ORCID iD

Bhagirathi Dash http://orcid.org/0000-0002-5314-5372

References

1. Catterall WA. Voltage-gated sodium channels at 60: structure, function and pathophysiology. *J Physiol* 2012; 590: 2577–2589
2. Dib-Hajj SD, Cummins TR, Black JA and Waxman SG. Sodium channels in normal and pathological pain. *Annu Rev Neurosci* 2010; 33: 325–347.
3. Amor V, Zhang C, Vainshtein A, Zhang A, Zollinger DR, Eshed-Eisenbach Y, Brophy PJ, Rasband MN and Peles E. The paranodal cytoskeleton clusters Na+ channels at nodes of Ranvier. *Elife* 2017; 6: e21392.
4. Garrido JJ, Giraud P, Carlier E, Fernandes F, Moussif A, Fache MP, Debanne D and Dargent B. A targeting motif involved in sodium channel clustering at the axonal initial segment. *Science* 2003; 300: 2091–2094.

5. Ho TS, Zollinger DR, Chang KJ, Xu M, Cooper EC, Stankewich MC, Bennett V and Rasband MN. A hierarchy of ankyrin-spectrin complexes clusters sodium channels at nodes of Ranvier. *Nat Neurosci* 2014; 17: 1664–1672.
6. Gasser A, Ho TS, Cheng X, Chang KJ, Waxman SG, Rasband MN and Dib-Hajj SD. An ankyrinG-binding motif is necessary and sufficient for targeting Nav1.6 sodium channels to axon initial segments and nodes of Ranvier. *J Neurosci* 2012; 32: 7232–7243.
7. Barry J, Gu Y, Jukkola P, O'Neill B, Gu H, Mohler PJ, Rajamani KT and Gu C. Ankyrin-G directly binds to kinesin-1 to transport voltage-gated Na+ channels into axons. *Dev Cell*. 2014; 28: 117–131.
8. Su YY, Ye M, Li L, Liu C, Pan J, Liu WW, Jiang Y, Jiang XY, Zhang X, Shu Y and Bao L. KIF5B promotes the forward transport and axonal function of the voltage-gated sodium channel Nav1.8. *J Neurosci* 2013; 33: 17884–17896.
9. Lewis TL Jr, Mao T, Svoboda K and Arnold DB. Myosin-dependent targeting of transmembrane proteins to neuronal dendrites. *Nat Neurosci* 2009; 12: 568–576.
10. Rey M, Vicente-Manzanares M, Viedma F, Yanez-Mo M, Urzainqui A, Barreiro O, Vazquez J and Sanchez-Madrid F. Cutting edge: association of the motor protein non-muscle myosin heavy chain-IIA with the C terminus of the chemokine receptor CXCR4 in T lymphocytes. *J Immunol* 2002; 169: 5410–5414.
11. Kim JH, Wang A, Conti MA and Adelstein RS. Nonmuscle myosin II is required for internalization of the epidermal growth factor receptor and modulation of downstream signaling. *J Biol Chem* 2012; 287: 27345–27358.
12. Bu Y, Wang N, Wang S, Sheng T, Tian T, Chen L, Pan W, Zhu M, Luo J and Lu W. Myosin IIb-dependent regulation of actin dynamics is required for N-methyl-D-aspartate receptor trafficking during synaptic plasticity. *J Biol Chem* 2015; 290: 25395–25410.
13. Ryu J, Liu L, Wong TP, Wu DC, Burette A, Weinberg R, Wang YT and Sheng M. A critical role for myosin IIb in dendritic spine morphology and synaptic function. *Neuron* 2006; 49: 175–182.
14. Marquèze-Pouey B, Martin-Moutot N, Sakkou-Norton M, Lévêque C, Ji Y, Cornet V, Hsiao WL and Seagar M. Toxicity and endocytosis of spinocerebellar ataxia type 6 polyglutamine domains: role of myosin IIb. *Traffic* 2008; 9: 1088–1100.
15. Getty AL, Benedict JW and Pearce DA. A novel interaction of CLN3 with nonmuscle myosin-IIB and defects in cell motility of Cln3(-/-) cells. *Exp Cell Res* 2011; 317: 51–69.
16. Jensen CS, Watanabe S, Rasmussen HB, Schmitt N, Olesen SP, Frost NA, Blanpied TA and Misonou H. Specific sorting and post-Golgi trafficking of dendritic potassium channels in living neurons. *J Biol Chem* 2014; 289: 10566–10581.
17. Hartman MA and Spudich JA. The myosin superfamily at a glance. *J Cell Sci* 2012; 125: 1627–1632.
18. Masters TA, Kendrick-Jones J and Buss F. Myosins: domain organisation, motor properties, physiological roles and cellular functions. *Handb Exp Pharmacol* 2017; 235: 77–122.
19. Sakamoto T, Wang F, Schmitz S, Xu Y, Xu Q, Molloy JE, Veigel C and Sellers JR. Neck length and processivity of myosin V. *J Biol Chem* 2003; 278: 29201–29207.
20. Leterrier C, Vacher H, Fache MP, d'Ortoli SA, Castets F, Autillo-Touati A and Dargent B. End-binding proteins EB3 and EB1 link microtubules to ankyrin G in the axon initial segment. *Proc Natl Acad Sci U S A* 2011; 108: 8826–8831.
21. Wei Q and Adelstein RS. Conditional expression of a truncated fragment of nonmuscle myosin II-A alters cell shape but not cytokinesis in HeLa cells. *Mol Biol Cell* 2000; 11: 3617–3627.
22. Rogers M, Zidar N, Kikelj D and Kirby RW. Characterization of endogenous sodium channels in the ND7-23 neuroblastoma cell line: implications for use as a heterologous ion channel expression system suitable for automated patch clamp screening. *Assay Drug Dev Technol* 2016; 14: 109–130.
23. John VH, Main MJ, Powell AJ, Gladwell ZM, Hick C, Sidhu HS, Clare JJ, Tate S and Trezise DJ. Heterologous expression and functional analysis of rat Nav1.8 (SNS) voltage-gated sodium channels in the dorsal root ganglion neuroblastoma cell line ND7-23. *Neuropharmacology* 2004; 46: 425–438.
24. Wittmack EK, Rush AM, Craner MJ, Goldfarb M, Waxman SG and Dib-Hajj SD. Fibroblast growth factor homologous factor 2B: association with Nav1.6 and selective colocalization at nodes of Ranvier of dorsal root axons. *J Neurosci* 2004; 24: 6765–6775.
25. Wittmack EK, Rush AM, Hudmon A, Waxman SG and Dib-Hajj SD. Voltage-gated sodium channel Nav1.6 is modulated by p38 mitogen-activated protein kinase. *J Neurosci* 2005; 25: 6621–6630.
26. Kondo T, Okada M, Kunihiro K, Takahashi M, Yaoita Y, Hosoya H and Hamao K. Characterization of myosin II regulatory light chain isoforms in HeLa cells. *Cytoskeleton (Hoboken)* 2015; 72: 609–620.
27. O'Brien JE, Sharkey LM, Vallianatos CN, Han C, Blossom JC, Yu T, Waxman SG, Dib-Hajj SD and Meisler MH. Interaction of voltage-gated sodium channel Nav1.6 (SCN8A) with microtubule-associated protein Map1b. *J Biol Chem* 2012; 287: 18459–18466.
28. Laedermann CJ, Abriel H and Decosterd I. Post-translational modifications of voltage-gated sodium channels in chronic pain syndromes. *Front Pharmacol* 2015; 6: 263.
29. Lemaillet G, Walker B and Lambert S. Identification of a conserved ankyrin-binding motif in the family of sodium channel alpha subunits. *J Biol Chem* 2003; 278: 27333–27339.
30. Montersino A, Brachet A, Ferracci G, Fache MP, Angles d'Ortoli S, Liu W, Rueda-Boroni F, Castets F and Dargent B. Tetrodotoxin-resistant voltage-gated sodium channel Nav 1.8 constitutively interacts with ankyrin G. *J Neurochem* 2014; 131: 33–41.

31. Ipsaro JJ, Huang L and Mondragon A. Structures of the spectrin-ankyrin interaction binding domains. *Blood* 2009; 113: 5385–5393.
32. Guzik-Lendrum S, Heissler SM, Billington N, Takagi Y, Yang Y, Knight PJ, Homsher E and Sellers JR. Mammalian myosin-18A, a highly divergent myosin. *J Biol Chem* 2013; 288: 9532–9548.
33. Jana SS, Kim KY, Mao J, Kawamoto S, Sellers JR and Adelstein RS. An alternatively spliced isoform of non-muscle myosin II-C is not regulated by myosin light chain phosphorylation. *J Biol Chem* 2009; 284: 11563–11571.
34. Bird JE, Takagi Y, Billington N, Strub MP, Sellers JR and Friedman TB. Chaperone-enhanced purification of unconventional myosin 15, a molecular motor specialized for stereocilia protein trafficking. *Proc Natl Acad Sci U S A* 2014; 111: 12390–12395.
35. Brown JA, Wysolmerski RB and Bridgman PC. Dorsal root ganglion neurons react to semaphorin 3A application through a biphasic response that requires multiple myosin II isoforms. *MBoC* 2009; 20: 1167–1179.
36. Hudmon A, Choi JS, Tyrrell L, Black JA, Rush AM, Waxman SG and Dib-Hajj SD. Phosphorylation of sodium channel Na(v)1.8 by p38 mitogen-activated protein kinase increases current density in dorsal root ganglion neurons. *J Neurosci* 2008; 28: 3190–3201.
37. Tan ZY, Piekarz AD, Priest BT, Knopp KL, Krajewski JL, McDermott JS, Nisenbaum ES and Cummins TR. Tetrodotoxin-resistant sodium channels in sensory neurons generate slow resurgent currents that are enhanced by inflammatory mediators. *J Neurosci* 2014; 34: 7190–7197.
38. Ho C, Zhao J, Malinowski S, Chahine M and O'Leary ME. Differential expression of sodium channel beta subunits in dorsal root ganglion sensory neurons. *J Biol Chem* 2012; 287: 15044–15053.
39. Bridgman PC, Dave S, Asnes CF, Tullio AN and Adelstein RS. Myosin IIB is required for growth cone motility. *J Neurosci* 2001; 21: 6159–6169.
40. Tullio AN, Bridgman PC, Tresser NJ, Chan CC, Conti MA, Adelstein RS and Hara Y. Structural abnormalities develop in the brain after ablation of the gene encoding nonmuscle myosin II-B heavy chain. *J Comp Neurol* 2001; 433: 62–74.
41. Rex CS, Gavin CF, Rubio MD, Kramar EA, Chen LY, Jia Y, Huganir RL, Muzyczka N, Gall CM, Miller CA, Lynch G and Rumbaugh G. Myosin IIb regulates actin dynamics during synaptic plasticity and memory formation. *Neuron* 2010; 67: 603–617.
42. Wang A, Ma X, Conti MA and Adelstein RS. Distinct and redundant roles of the non-muscle myosin II isoforms and functional domains. *Biochem Soc Trans* 2011; 39: 1131–1135.
43. Ma X, Kawamoto S, Hara Y and Adelstein RS. A point mutation in the motor domain of nonmuscle myosin II-B impairs migration of distinct groups of neurons. *MBoC* 2004; 15: 2568–2579.
44. Pei Z, Pan Y and Cummins TR. Posttranslational modification of sodium channels. *Handb Exp Pharmacol* 2018; 246: 101–124.
45. Onwuli DO and Beltran-Alvarez P. An update on transcriptional and post-translational regulation of brain voltage-gated sodium channels. *Amino Acids* 2016; 48: 641–651.
46. Tumbarello DA, Kendrick-Jones J and Buss F. Myosin VI and its cargo adaptors – linking endocytosis and autophagy. *J Cell Sci* 2013; 126: 2561–2570.
47. Kneussel M and Wagner W. Myosin motors at neuronal synapses: drivers of membrane transport and actin dynamics. *Nat Rev Neurosci* 2013; 14: 233–247.
48. Zhou D, Lambert S, Malen PL, Carpenter S, Boland LM and Bennett V. AnkyrinG is required for clustering of voltage-gated Na channels at axon initial segments and for normal action potential firing. *J Cell Biol* 1998; 143: 1295–1304.
49. Gee SH, Madhavan R, Levinson SR, Caldwell JH, Sealock R and Froehner SC. Interaction of muscle and brain sodium channels with multiple members of the syntrophin family of dystrophin-associated proteins. *J Neurosci* 1998; 18: 128–137.
50. Allouis M, Le Bouffant F, Wilders R, Peroz D, Schott JJ, Noireaud J, Le Marec H, Merot J, Escande D and Baro I. 14-3-3 is a regulator of the cardiac voltage-gated sodium channel Nav1.5. *Circ Res* 2006; 98: 1538–1546.
51. Sato PY, Musa H, Coombs W, Guerrero-Serna G, Patino GA, Taffet SM, Isom LL and Delmar M. Loss of plakophilin-2 expression leads to decreased sodium current and slower conduction velocity in cultured cardiac myocytes. *Circ Res* 2009; 105: 523–526.